VOLUME 1, NUMBER 10, OCTOBER 2001

NANO LETTERS

Control of Dewetting Dynamics by Adding Nanoparticle Fillers

S. Sharma,*,† M. H. Rafailovich,† D. Peiffer,‡ and J. Sokolov†

Department of Materials Science and Engineering, State University of New York at Stony Brook, Stony Brook, New York 11733, and Exxon/Mobil Research and Engineering Co., East Clinton Township, Annandale, New Jersey 08801

Received June 14, 2001; *Revised Manuscript Received August 6, 2001*

ABSTRACT

Producing a stable polymer film is a challenge, because dewetting tends to rupture the film. To overcome this drawback, it is essential to control the factors responsible for stabilizing polymer films during processing. Here, we report on a unique strategy to control the rate of dewetting by dispersion of small amount of carbon black and colloidal Si nanoparticle fillers in the polymer thin film. Optical microscopy, AFM and TEM have been used to study the surface and interfacial structure in the vicinity of growing holes. The rate of dewetting is drastically different when filler particles are added to the polymer and strongly depends on nanoparticle concentration in the film. Even though the particle sizes are similar, their effects on the dynamics are very different. We explain our findings in the form of interaction between the polymer chains and particle surface.

Polymer bilayer films have numerous technological applications such as disk head lubricants, dielectric and optical coatings, lithographic resist layers, and electronic packaging.[1] Since most polymers are immsicible, bilayer films tend to be unstable against rupture and phase segregation. Consequently, dewetting of bilayer polymer films has been an area of intensive study in recent years.[2]

Recently, inorganic fillers are also being added to the polymer films in order to improve their mechanical response or engineer special electronic and optical properties.[3,4] The amount of filler added is usually small, and the filler is inert and does not react with the polymer to alter chemical properties, such as surface tension or the Flory interaction parameter. Hence, not much attention has been given to the effect of fillers on film stability, which is governed only by known differences in the surface and interfacial energy of the polymers. Recently Karim and co-workers[4] have shown that the addition of C can stabilize homopolymer films against dewetting by segregating to the substrate and on a substrate by pinning the polymer chains. We will concentrate in this paper on the effects of filler particles on dewetting characteristics of thin films. The system we chose to study, PS and PMMA, is well characterized and the dewetting properties of the unfilled bilayer films[5] are well-known. Furthermore, the fillers we will introduce, carbon black and colloidal Si, are common components in polymer composites.

Sample Preparation Techniques. Monodisperse polystyrene (PS), Mw = 123 K Mw/Mn = 1.4 and poly(methyl methacrylate)(PMMA) of Mw = 125 K and Mw/Mn = 1.02 were chosen for this study. The silicon wafers used in the experiment were cleaned by a regular cleaning process. Since

* Corresponding author.
† SUNY.
‡ Exxon/Mobil Research and Engineering Co.

10.1021/nl0100466 CCC: $20.00
Published on Web 08/29/2001

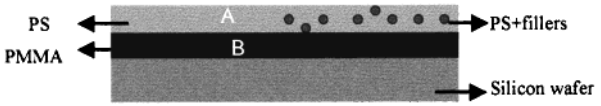

Figure 1. Schematic illustration of the sample showing two separate PS films, with and without nanoparticles, floated on top of a 28-nm thick PMMA film on a spun cast film on a Si wafer.

PMMA is preferentially adsorbed to the Si substrate, a thin film, 280 Å thick, was spun cast directly onto the substrate. The thickness of this film was chosen such that we can measure the Young's contact angle between the PS droplets and the substrate after completion of the dewetting. CB (330) and colloidal Si at a concentration of 0.01 wt % were added to monodisperse PS Mw= 123 K. Silica particles were pyrogenous silica Aerosil 300, with primary particle size of 90 Å and specific surface area of 295 m^2/g. The solutions of the nanoparticles and polymer appeared clear, indicating that the particles were well dispersed.

The PS solution with particles was spun cast onto glass slides and carefully floated off deionized water onto half of the PMMA covered Si substrate. Another PS film of the same thickness and Mw, but without particles, was also spun cast and floated from the water bath onto the adjacent half of the PMMA substrate. This sample geometry (Figure 1) was chosen such that the dewetting of the two films occurred under nearly identical conditions. Dewetting was initiated by annealing the samples in a vacuum oven at a pressure of 10^{-7} Torr for different times at $T = 165$ °C and $T = 162$ °C for the Si and CB particles, respectively.

For a polymer bilayer film composed of two immiscible liquids, such as the one shown in Figure 1, dewetting is controlled by the spreading parameter, S, which quantifies the balance between minimizing interfacial area and presenting the polymer with the lowest surface tension at the vacuum interface.[6] The spreading parameters can be expressed in terms of γ_B, γ_A, and γ_{AB}, which are, respectively, the surface tensions of PMMA, PS, and the interfacial tension between the two polymers:

$$S = \gamma_B - (\gamma_A + \gamma_{AB}) \quad (1)$$

Wetting and dewetting occur when $S < 0$ or $S > 0$, respectively.

In order for the dewetting process to begin, holes are either nucleated around defects, or if the films are less than several hundred nanometers, the holes are initiated by capillary waves.[7] When $S < 0$, dewetting continues and the holes grow with a constant velocity, V, given by

$$V = |S|/\theta^3 e/\eta_A \quad (2)$$

where η_A is the viscosity of PS and θ is the Neumann angle. With increasing annealing time, the holes become large enough so their rims contact each other forming unstable ribbons, which decay into isolated droplets.

This process is illustrated in Figure 2a for the control of the PS/PMMA bilayer sample without the particles. Prior to annealing, the surface of the sample was uniform. For this polymer system $S < 0$, and hence when the sample was

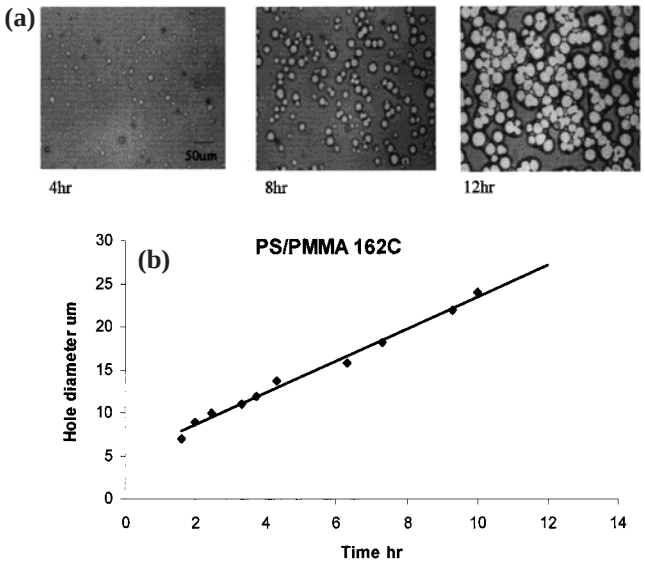

Figure 2. (a) Optical micrograph of the surface showing the evolution of an area as a function of annealing time. The film was composed of homopolymer with filler particles. (b) Graph of hole diameter vs time for 123 K PS annealed at 162 °C.

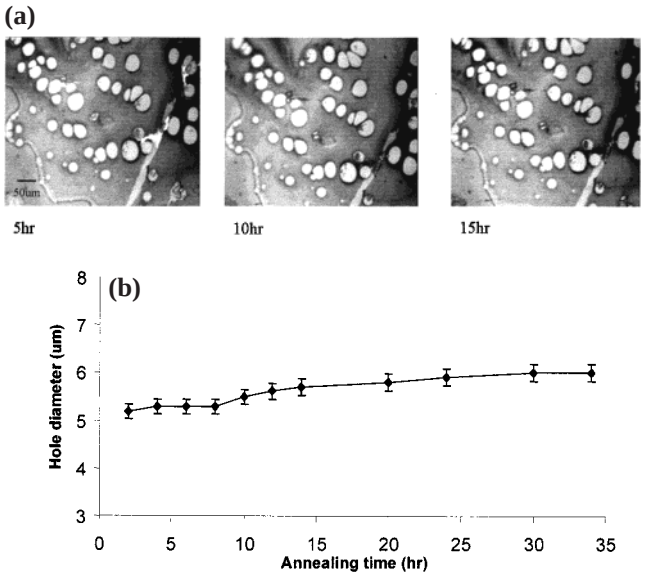

Figure 3. (a) Optical micrograph of same area of 123 K PS without silica particles for three different annealing times at 162 °C. (b) Graph of hole diameter vs time for 123 K PS with Si particles annealed at 165 °C.

annealed at $T = 162$ °C (above T_g for both polymers) dewetting was initiated. From Figure 2a we see that after 4 h of annealing holes with well-defined rims have begun to form. The development of the holes in the same area of the sample as a function of annealing is shown in the subsequent figures. In Figure 2b we plot the average diameter of the holes as a function of time. From the figure we can see that the relationship is linear and the process is as predicted.[8]

The situation is drastically different when filler particles are added to the PS layer. Figure 3a is an optical micrograph of the bilayer sample containing Si particles. From the figure we can see that large holes are present even prior to annealing. Annealing the samples for up to 32 h produces

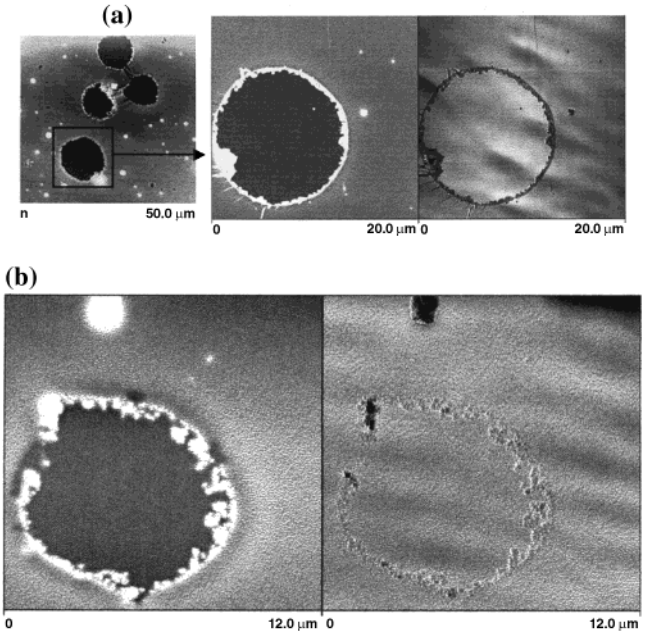

Figure 4. (a) AFM scan of several holes on the PS surface with Si particles. The topographical and lateral force images of a hole prior to annealing. The particles are clearly seen in the lateral force image where they appear darker than the surrounding polymer. (b) AFM scan of the same hole after annealing for 24 h. The particle clusters in the rim are now clear. The size of the clusters is approximately 100 nm.

negligible change in the image, in either the size or the number of holes. This is also confirmed in Figure 3b, where we plot the diameter as a function of time. Comparing to Figure 2b, we see that the change is very small.

To obtain a more detailed view, the samples were also analyzed with atomic force microscopy (AFM) in the contact mode. The topographical and lateral force images of a hole prior to annealing are shown in Figure 4a. From the topographical figure we see that the rim appears slightly irregular and seems to be composed of particle clusters. The particles are clearly seen in the lateral force image where they appear darker (i.e., harder) than the surrounding polymer. Furthermore, no contrast is seen between the exposed polymer at the center of the hole and in the overlying film. This in contrast to the images shown by S. Qu[5] where the exposed PMMA always appears darker relative to the PS film. Cross sectional analysis of the hole indicates that it is only 23 nm deep, which is less than the total PS film thickness of 28 nm. Hence the film seems to rupture before the PMMA interface is reached, which is consistent with the lack of lateral force contrast. This was further confirmed using TOF−SIMS imaging analysis where no oxygen is detected in the hole area, indicating that the PMMA interface is not yet exposed. Figure 4b shows the same hole after annealing for 24 h. From the figure we see that the particle nature of the rim is now clear and the individual clusters appear. The diameter of the clusters is approximately 100 nm, which is consistent in with neutron scattering data.[9] The contrast of the particles is no longer visible in the lateral force image, indicating that they are now covered with a PS layer.

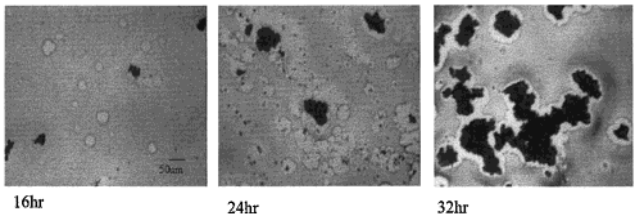

Figure 5. Optical images of the bilayer sample containing carbon black annealed at 162 °C for three different annealing times. Initially there is a normal pattern of hole development, but after further annealing holes are no longer round, and micron scale clusters of carbon black appear at the center of some of the holes.

Observation of the optical and AFM micrographs of the holes clearly shows that no polymer rim is apparent even though the holes are fairly large. We can therefore conclude that no viscous flow as described by eq 2 has occurred. This is consistent with the fact that the holes are formed well below T_g of the films where center of mass motion of the polymers is very slow. Therefore, the holes must be due to spontaneous rupture of the film due to relieve strain induced by the particle clusters, which are large compared to the total film thickness. Once the strain is relaxed, no further holes are formed. Upon bursting, the particle clusters appear to migrate to the rim of the hole where they seem to pin the contact line, preventing further growth. Growth does not occur even when the film is annealed above its glass transition, where viscous flow can occur. It is known from previous diffusion studies that the interaction between PS and Si surfaces can be very strong. In fact, Zheng[10] has shown that the diffusion coefficient for a polymer layer adjacent to the interface can be reduced by several orders of magnitude. Hence, this interaction may also be present between the PS and particles that can pin the hole and prevent viscous motion of the hole rim above T_g.

Optical images of the bilayer sample containing carbon black are shown in Figure 5. From the figure we can see that initially there is a normal pattern of hole development and growth which is analogous to the sample without filler shown in Figure 2a. The AFM images are uneventful and no particle clusters are visible. After prolonged annealing for 16 h or longer, we begin to notice that the holes are no longer round and large; micron-scale clusters of carbon black appear at the center of some of the holes. As annealing progresses, the growth of the holes is no longer regular. The accumulation of carbon black in the holes increases, distorting the pattern and producing significant roughness. Furthermore, additional holes begin to open, as shown in the lower magnification micrograph in Figure 6a. The number of holes, rather than the diameter, is now seen to grow linearly with time (Figure 6b). Careful examination of the micrograph after 32 h of annealing shows that carbon black clusters avoid the interface with the PS polymer. The morphology of the film indicates that phase separation is now occurring between the PS and the carbon black where the carbon black phase is segregated into the center of the holes. Similar behavior was observed with other carbon black concentrations. Increasing the concentration did not affect the dewetting velocity; rather, as shown in Figure 7, the

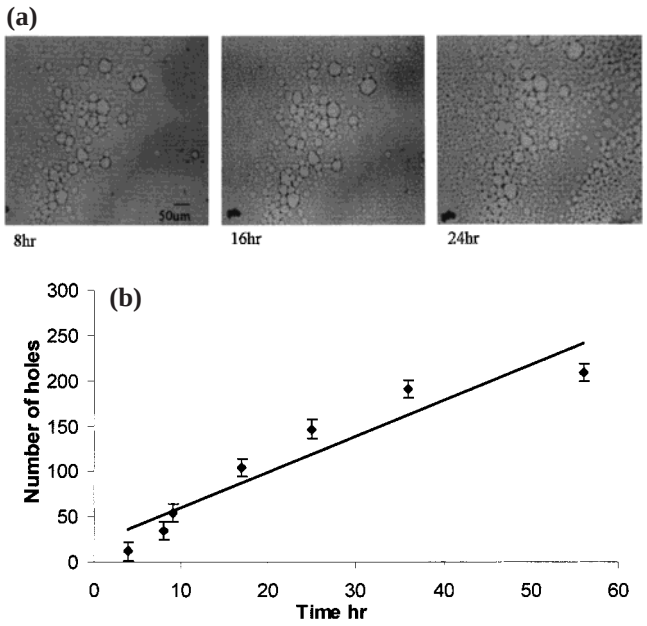

Figure 6. (a) Optical micrograph showing additional holes beginning to open with increase in annealing time. (b) Graph of number of holes vs time for carbon black at 162 °C.

number of holes increases linearly with concentration. This can be interpreted simply by assuming that holes can form more readily with increasing initial concentration.

In conclusion, we have shown that the addition of filler particles can have a dramatic effect on the nature of dewetting in a polymer bilayer film. When the interaction between the polymer and the particles is strong, as is the case between the Si particles and PS, dewetting is arrested. AFM images clearly show the distribution of particles at the edge of the holes, indicating that interfacial pinning is the probable mechanism. When an unfavorable interaction exists between the particle and the polymer, as is the case for PS and carbon black, phase separation of the particles from the polymer and dewetting of the bilayer films proceed simultaneously. Hence, a repulsive interaction further destabilizes the films and increases the rate and magnitude of dewetting.

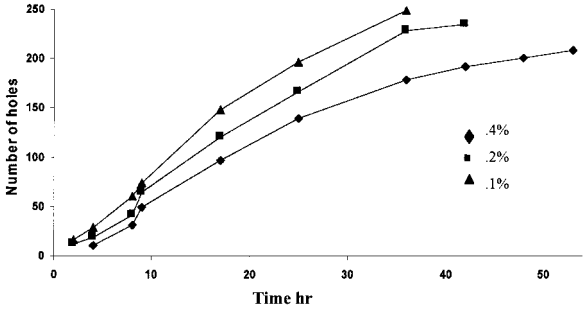

Figure 7. Graph of number of holes vs time for various concentrations.

In these studies the particle sizes were large compared to the film thickness, and hence the initial morphologies were complicated by strain release. Further studies are in progress where uniform nanoscale particles are used and the effects of polymer/particle interactions can be separated from elastic strain release.

References

(1) Siegel, R. W. *Mater. Sci. Eng. A* **1993**, *168*, 189.
(2) Martin, P.; Buguin, A.; Brochard-Wyart, F. *Europhys. Lett.* **1994**, *28*, 421.
(3) McMicheal, R. D.; Shull, R. D.; Swartzendruber, L. J.; Bennett, L. H. *Magn. Mater.* **1992**, *129*, 134.
(4) Feng, Y.; Karim, A.; Weiss, R. A.; Douglas, J. F.; Han, C. C. *Macromolecules* **1998**, *31*, 484.
(5) Qu, S.; Clark, C. J.; Liu, Y.; Sokolov, J.; Rafailovich, M. H.; *Macromolecules* **1997**, *30*, 3640−3645.
(6) Lambooy, P.; Phelan, K. C.; Haugg, O.; Krausch, G. *Phys. Rev. Lett.* **1996**, *76*, 1110.
(7) Redon, C.; Brochard-Wyart, F.; Rondelez, F. *Phys. Rev. Lett.* **1991**, *66*, 71.
(8) Sharma, S.; Rafailovich, M. H.; Sokolov, J.; Liu, Y.; Qu, S.; Schwarz, S. A.; Eisenberg, A. *High Perform. Polym.* **2000**, *12* (4), 581−586.
(9) Yimin Zhang, Thesis, SUNY at Stony Brook, May, 2001.
(10) Zheng, X.; Rafailovich, M. H.; Sokolov, J.; Strzhemechny, Y.; Schwarz, S. A.; Sauer, B. B.; Rubinstein, M. *Phys. Rev. Lett.* **1997**, *79*, 241.

NL0100466